An Analytical View of Updating Meteorological Variables: Part I. Phase Errors

WILLIAM BLUMEN

Dept. of Astro-Geophysics, University of Colorado, Boulder 80302

(Manuscript received 18 March 1974, in revised form 14 September 1974)

ABSTRACT

Truncation error and, possibly, inadequate parameterization of physical processes, cause the propagation speed of atmospheric disturbances to be generally underestimated by numerical atmospheric models. Updating meteorological variables in a model with atmospheric data may improve its predictive capability, but a significant root mean square error will remain. The contribution to this error, due to differences in phase between atmospheric and model disturbances, is analyzed by means of a simple linear model that permits gravity-interia wave propagation superposed on a more slowly evolving quasi-geostrophic flow. Model pressure or wind variables are updated with control data, designed to simulate real data assimilation. Under this circumstance, the model fields of pressure or wind will always differ from the control fields. As the number of updates increases, this difference approaches an asymptotic error that depends only on the characteristic spatial scale of the wave disturbance and the difference in phase between the model and control disturbances. For scales of motion characteristic of mid-latitude synoptic-scale flow, this asymptotic error is essentially reached after four to seven updates with the control field. The asymptotic error level will be increased, however, if the phase error varies with time in a more or less random manner or if the disturbance flow has a spatially varying amplitude. As a corollary, when phase errors exist between the observed and model states, it is shown that asynoptic data assimilation, carried out on a random basis, increases the asymptotic error by the addition of random noise error. Some of the results are in agreement with Williamson's numerical experiments, while others have not been tested.

Error reduction appears to be attainable, for mid-latitude flow, if truncation error associated with the principal energy bearing modes can be controlled. However, it does not appear that updating tropical flow will yield significant error reduction because energy is distributed over a broader spectral range and, consequently, truncation error would be more difficult to control.

1. Introduction

Numerical prediction models of the earth's atmosphere are designed to produce the best possible forecast of meteorological fields from specified initial data, say, pressure, temperature and wind velocity. It is recognized that severe constraints, imposed on these models, have provided limitations on the forecast accuracy that can be attained. It appears that the most serious obstacle to the improvement of short-range forecasting ($\lesssim$72 h) at the present time is the lack of sufficiently detailed observational coverage in space and time. This information is needed to supply initial conditions to start the integration, to update the initial conditions during the course of the integration and, finally, to provide a quantitative verification measure to test the models' performance. In the case of longer range forecasting or general circulation modelling, many additional physical processes have to be included in a model. Here it is critically important to have adequate global observational coverage in order to be able to judge the performance of a model in terms of the various parameterizations of physical processes that are usually incorporated.

Technology has made available satellite and balloon-based observing systems that appear to be capable of providing, in the near future, a major portion of the four-dimensional data required for the more efficient use of current and planned numerical models. Because of this potential boon to the present observational network, a broadly based research effort is underway, with the expressed purpose of establishing a more precise statement of the data requirements and how such requirements can be achieved at the lowest cost and with a minimum of data redundancy. The paths and progress of this research have been well-stated in recent articles by Kasahara (1972) and Jastrow and Halem (1973).

It appears that to attain the goals, delineated above, researchers have resorted almost entirely to numerical experimentation—on a more or less trial and error basis—with far less guidance from theoretical principles than has characterized the past development of numerical models. This paper represents an attempt to pinpoint a particular and important aspect of *four-dimensional data assimilation* or, more simply, *updating*, and to examine this problem analytically by means of a simple model in order to isolate and evaluate the rela-

tive importance of the essential parameters of the problem.

To be specific, at least three deleterious problems have to be surmounted before four-dimensional data assimilation proves to be a viable adjunct to numerical prediction. First, the insertion of real observations into a less-than-perfect model provides data which generally will differ from the field produced by the model at that time. As a consequence of the mass and momentum inbalances interjected and the fact that the model physics generally differs from real atmospheric dynamics, large imbalances can be introduced at a particular time. This is not a realistic atmospheric state and, according to Jastrow and Halem (1973), this effect will emerge as the major source of forecast error when real data insertion is attempted. More recent experiments by Hayden (1973) suggest that it is possible to control the disturbance level or initial "shock" by judicious smoothing or balancing procedures. Kasahara (1972) has presented a brief survey of a number of these assimilation procedures. At this point the problem has not been satisfactorily solved, but the tenor, as expressed in recent work, promotes the feeling that the problem is coming under control.

The second problem is referred to as "predictability error growth." Principally, the nonlinear interactions described by the model dynamics spread initial errors throughout the spectrum of allowable motions. As a consequence, the model solution diverges from the true atmospheric state until the forecast value of the model loses significance. (Predictability error growth is well-demonstrated by comparing the divergence of two solutions of the same model started from small differences in the initial conditions.) Numerical experiments by Williamson and Kasahara (1971) and Williamson (1973), for example, indicate that updating the model with control data, to simulate an atmospheric observed state, may lead to significant error reduction and in some cases, may reduce the error to within the tolerable data limitations set for the First GARP Global Experiment (FGGE).

Kasahara (1972) and Williamson (1973) have pointed up a third source of error, one arising from truncation errors inherent in the particular numerical algorithms used to solve the model equations. Williamson displays the effect of this error, by updating a course resolution model (5° grid interval) with data generated by the same model, but using a finer mesh (2.5° grid interval). This experiment is intended to simulate real data assimilation. The error growth is rapid and the asymptotic error level reached is a factor of 5 to 10 higher than the asymptotic error level associated with predictability error growth alone. These features are displayed in Figs. 1 and 2, from Williamson (1973), using the NCAR Global Circulation Model. Moreover, Williamson found that periodic updating of the 5° model with data taken from the 2.5° model only reduced the asymptotic rms error, representing the difference between randomly

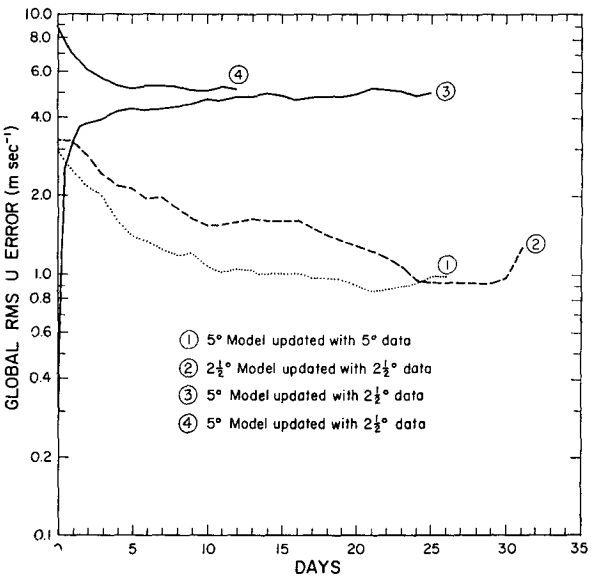

FIG. 1. Global rms wind error resulting from updating temperature and surface pressure every 12 h, using the NCAR GCM.

chosen states of the model, by a factor of 2. As a result, this experiment suggests that truncation error may, indeed, turn out to be the most important source of forecast error when real data are assimilated into a numerical prediction model. The present paper is addressed to this error alone.

The basic working hypothesis is that the principal contribution to the rms error, due to truncation, arises because the propagation speed of weather systems is generally underestimated by numerical models. Some numerical differencing schemes overestimate the propa-

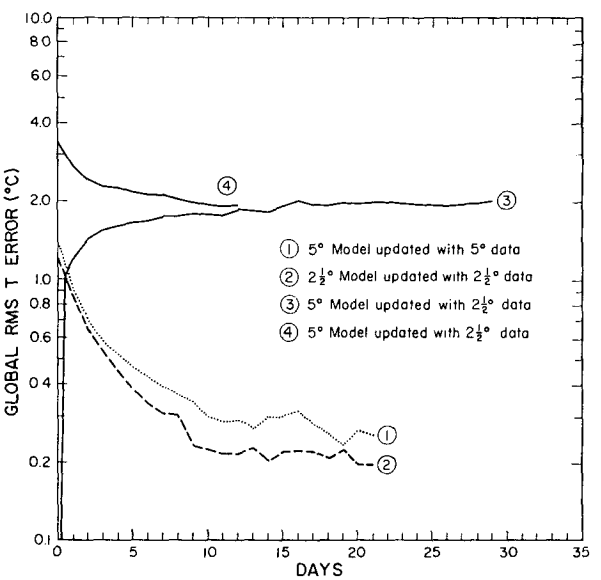

FIG. 2. Global rms temperature error resulting from updating wind every 12 h, using the NCAR GCM.

gation speed, but this detail does not affect the stated premise. The alteration of the phase speed of wave disturbance is a well-established theoretical deduction underscored by Kurihara (1965), among others. Miyakoda *et al.* (1971, 1972) have compared observed propagation speeds with those produced by the GFDL General Circulation Model, using different grid intervals. These comparisons show that spurious propagation of disturbances is a function of the grid interval used, although the relationship is not simply explained.

The model to be used in the present study is introduced in Section 2. Application of the model to data assimilation, along the lines developed by Williamson and Dickinson (1972), appears in Section 3. The analysis is further developed, in Sections 4 and 5, to include phase differences between the model solutions and a "control" state; additional errors that arise when these phase differences are randomly distributed in time, or when a varying amplitude is introduced, are then examined in Sections 6 and 7. A summary and some final remarks concerning error reduction by updating meteorological variables are contained in Section 8.

2. Model characteristics and solutions

a. Model

A shallow-water model will be employed for present computational purposes. Its atmospheric analogue is a barotropic model with depth-independent divergence that permits surface pressure changes to occur. The development of the model equations, that serve present purposes, has been presented in detail by Blumen (1972). Briefly, it is noted that the observed atmospheric state is generally close to hydrostatic-geostrophic balance. Superposed on this state are gravity-inertia waves, containing relatively little energy, whose characteristic time scale is about one order of magnitude smaller than the characteristic scale associated with the evolution of the more significant meteorological fields. The parameter that expresses the ratio of these periods is the Rossby number

$$\mathrm{Ro}=U_0/(f_0L), \tag{1}$$

where the fast time scale is $T\sim f_0^{-1}$ (f_0 is the Coriolis parameter) and the slow time scale is $\tau\sim LU_0^{-1}$ (L and U_0 are the characteristic horizontal scale and velocity amplitude of the quasi-geostrophic field). In mid-latitudes, Ro is characteristically order 10^{-1}. As a consequence, the multiple time-scale approach (e.g., Cole, 1968) may be used to determine a consistent expansion, in Ro, for the development of a set of equations governing *both* the gravity inertia wave dependence on the fast time T and the quasi-geostrophic evolution on a time scale τ.

The nondimensionalization of the basic equations proceeds from

$$\left.\begin{aligned}&(u_*,v_*)=U_0(u,v),\quad (x_*,y_*)=L(x,y),\quad t_*=f_0^{-1}t\\&gh_*/(gD_0)=(f_0U_0L/gD_0)\pi=\lambda^{-2}\,\mathrm{Ro}\pi\\&f=f_0[1+(\beta_*L^2/U_0)\,\mathrm{Roy}]=f_0(1+\beta\,\mathrm{Roy})\end{aligned}\right\}, \tag{2}$$

where (u_*,v_*) are (x_*,y_*) velocity components, positive to the east and north, respectively; t_* denotes time and h_* is the free surface height deviation from the constant undisturbed depth D_0; g is the acceleration of gravity per unit mass; $\beta_*=df/dy=$constant; and the parameter λ is the nondimensional Rossby radius of deformation

$$\lambda=(gD_0)^{\frac{1}{2}}f_0^{-1}L^{-1}. \tag{3}$$

We have also defined

$$\left.\begin{aligned}&T=t\\&\tau=\mathrm{Ro}t\end{aligned}\right\}. \tag{4}$$

The zero-order terms in the expansion are

$$\partial u_0/\partial T-v_0+\partial\pi_0/\partial x=0, \tag{5}$$

$$\partial v_0/\partial T+u_0+\partial\pi_0/\partial y=0, \tag{6}$$

$$\partial\pi_0/\partial T+\lambda^2(\partial u_0/\partial x+\partial v_0/\partial y)=0. \tag{7}$$

The zero-order dependence on the slow time τ is found by going to the first-order terms. The condition that ensures that the expansion procedure is uniformly valid out to the slow time is

$$\left(\frac{\partial}{\partial\tau}+U\frac{\partial}{\partial x}+V\frac{\partial}{\partial y}\right)\Omega_0=0, \tag{8}$$

where $U(x,y,\tau)$ and $V(x,y,\tau)$ are zero-order geostrophic velocities, defined by $U=-\partial\Pi/\partial y$, and $V=\partial\Pi/\partial x$, and Π denotes the geostrophic height field; the potential vorticity $\Omega_0(x,y,\tau)$ is defined as

$$\Omega_0=\Delta\Pi-\lambda^{-2}\Pi+\beta y \tag{9}$$

($\Delta=\partial^2/\partial x^2+\partial^2/\partial y^2$). The complete zero-order disturbance field is represented by

$$\left.\begin{aligned}u_0&=U(x,y,\tau)+u(x,y,T,\tau)\\v_0&=V(x,y,\tau)+v(x,y,T,\tau)\\\pi_0&=\Pi(x,y,\tau)+\pi(x,y,T,\tau)\end{aligned}\right\}, \tag{10}$$

and the potential vorticity of the ageostrophic flow is identically zero:

$$\partial v/\partial x-\partial u/\partial y-\lambda^{-2}\pi\equiv 0. \tag{11}$$

The wave equation governing the ageostrophic flow may be derived from (5), (6) and (7), using (10) and (11). We obtain

$$\left(\frac{\partial^2}{\partial T^2}+1-\lambda^2\Delta\right)\pi=0. \tag{12}$$

This wave equation (12) and the *quasi-geostrophic fore-*

cast equation (8) constitute the basic equations of this study.

The physical process described by this system is one of adaptation to geostrophic balance within a characteristic time T with concurrent evolution of the geostrophic field occurring over a longer period τ. In essence, this model permits both processes to occur simultaneously in contradistinction to usual approaches, whereby each physical process is treated as an independent phenomenon. Three initial conditions are required to determine the arbitrary constants arising in the solutions of (8) and (12). These are given, to zero-order, by

$$\pi_0=\Pi(x,y,0)+\pi(x,y,0,0)=\pi_i(x,y), \tag{13}$$

$$\frac{\partial\pi_0}{\partial T}=\frac{\partial\pi_i}{\partial T}, \tag{14}$$

$$\frac{\partial^2\pi_0}{\partial T^2}=\frac{\partial^2\pi_i}{\partial T^2}, \tag{15}$$

where $\pi_i(x,y)$ represents the observed or specified initial value of the π_0 field. Since the geostrophic value Π is independent of the fast time T, the left-hand sides of (14) and (15) may be replaced by $\partial\pi/\partial T$ and $\partial^2\pi/\partial T^2$. Moreover, if use is made of (5), (6) and (7), conditions (14) and (15) may be expressed as

$$\frac{\partial\pi(x,y,0,0)}{\partial T}=-\lambda^2\left(\frac{\partial u_i}{\partial x}+\frac{\partial v_i}{\partial y}\right), \tag{16}$$

$$\frac{\partial^2\pi(x,y,0,0)}{\partial T^2}=-\lambda^2\left(\frac{\partial v_i}{\partial x}-\frac{\partial u_i}{\partial y}-\Delta\pi_i\right). \tag{17}$$

Note, however, that the ageostrophic field π may be a function of the slow time τ. We shall return to this point when the wave solutions are presented.

The energy equation for the zero-order disturbance field will now be considered. It is shown in the Appendix that

$$\frac{\partial}{\partial T}\frac{1}{2}\int\int_S(u_0^2+v_0^2+\lambda^{-2}\pi_0^2)dxdy=0, \tag{18}$$

where S denotes the region encompassing the flow and the normal velocity is assumed to vanish on the boundaries of S. If (10) is introduced into (18), a cross-product term arises. Upon integration by parts, this term may be expressed as

$$\int\int_S(Uu+Vv+\lambda^{-2}\Pi\pi)dxdy$$

$$=-\int\int_S\Pi\left(\frac{\partial v}{\partial x}-\frac{\partial u}{\partial y}-\lambda^{-2}\pi\right)dxdy. \tag{19}$$

However, this cross-product term vanishes identically, by (11). Consequently, Eq. (18) may be expressed as

$$\frac{1}{2}\int\int_S[U^2+V^2+\lambda^{-2}\Pi^2+u^2+v^2+\lambda^{-2}\pi^2]dxdy=\mathcal{E}(\tau), \tag{20}$$

where $\mathcal{E}(\tau)$ is a function of τ. It is shown in the Appendix that

$$\frac{\partial}{\partial\tau}\frac{1}{2}\int\int_S[U^2+V^2+\lambda^{-2}\Pi^2+u^2+v^2+\lambda^{-2}\pi^2]dxdy=0. \tag{21}$$

As a result, $\mathcal{E}(\tau)=\mathcal{E}(\tau=T=0)$. Moreover, the energy equation for the quasi-geostrophic flow may be derived by multiplying (8) by Π and integrating over S. We obtain

$$\frac{\partial}{\partial\tau}\frac{1}{2}\int\int_S(U^2+V^2+\lambda^{-2}\Pi^2)dxdy=0. \tag{22}$$

Comparison of (21) and (22) shows that

$$\frac{\partial}{\partial\tau}\frac{1}{2}\int\int_S(u^2+v^2+\lambda^{-2}\pi^2)dxdy=0. \tag{23}$$

Then (22) and (23) imply that the initial conditions determine the energy partition between the geostrophic and ageostrophic components; thereafter each component conserves this energy throughout the period of flow, although nonlinear interactions between the geostrophic modes is permitted by (8). It is necessary to go to higher order in the expansion process to find interactions between the ageostrophic and geostrophic motions.

b. Solutions

A solution of (12) consisting of two Fourier components, representing waves travelling in opposite directions, is given by

$$\pi=[A_1e^{i(kx+\omega T)}+A_2e^{i(kx-\omega T)}]e^{ily}, \tag{24}$$

where k, l are x, y wavenumbers, A_1 and A_2 are arbitrary functions of τ, to be determined, and

$$\omega^2=1+\lambda^2(k^2+l^2). \tag{25}$$

The *nonlinear* forecast equation (8) is satisfied by the Craig (1945)–Neamtan (1946) solution

$$\Pi=-Uy+Be^{i(kx+\sigma\tau)+ily}, \tag{26}$$

where U is a constant zonal flow, B is a constant to be

determined, and

$$\sigma=-k[U(k^2+l^2)-\beta]/(k^2+l^2+\lambda^{-2}). \tag{27}$$

The functions A_1 and A_2, appearing in (24), are only functions of slow time τ. The expressions for A_1 and A_2 are determined in a manner which is similar to the development leading to condition (8). However, in the present study, there is no need to determine A_1 and A_2. Use will only be made of (24) at the initial time or at that time when data is assimilated. Once the arbitrary constants $A_1(0)$, $A_2(0)$ and B are determined, the gravity waves will be removed from the solution. The basis for this step will be discussed in Section 3. It is sufficient to say that this step *cannot* be taken if the zero-order gravity-wave amplitude grows with time. However, the energy equation (23) ensures that A_1 and A_2 remain bounded, because there is no energy source available for finite-amplitude growth.

The constants $A_1(0)$, $A_2(0)$ and B are determined from the initial conditions (13), (16) and (17). We define

$$\left.\begin{aligned} D&=\frac{\partial u_i}{\partial x}+\frac{\partial v_i}{\partial y}\\ Z&=\frac{\partial v_i}{\partial x}-\frac{\partial u_i}{\partial y}-\Delta\pi_i\\ &=\Delta(\psi_i-\pi_i)\end{aligned}\right\}, \tag{28}$$

where $\psi_i(x,y)$ is the streamfunction of the initial flow. From (16), (17) and (24) we obtain

$$\left.\begin{aligned} A_1-A_2&=-\lambda^2\hat{D}\omega^{-1}\\ A_1+A_2&=\lambda^2\hat{Z}\omega^{-2}\end{aligned}\right\}, \tag{29}$$

where the circumflex denotes the amplitude of D and Z, and ω is given by (25). A_1 and A_2 may easily be determined from (29) to yield

$$\pi|_{\tau=T=0}=\frac{\lambda^2}{\omega^2}\hat{Z}e^{i(kx+ly)}. \tag{30}$$

Next, we specify the initial state as

$$\pi_i(x,y)=-Uy+\hat{\pi}_i e^{i(kx+ly)}, \tag{31}$$

where $\hat{\pi}_i$ is a constant. Finally, we introduce (26), (30) and (31) into (13), to obtain

$$B=\hat{\pi}_i-\frac{\lambda^2}{\omega^2}\hat{Z}. \tag{32}$$

The solution for Π is

$$\Pi(x,y,\tau)=-Uy+\left(\hat{\pi}_i-\frac{\lambda^2}{\omega^2}\hat{Z}\right)e^{i(kx+\sigma\tau)+ily}. \tag{33}$$

Frequent reference to (33) will be made in the following sections.

It is not necessary to assume simple solutions of the type (24) and (26) to validate the present analysis. A Fourier integral representation may be used in place of (24) and a more general solution for Π may be taken, if one can be found. This appears, however, to be an unnecessary complication at the present stage of the analyses. The simpler approach avoids undue computational complexity and, it is felt, captures the essence of the problem under study.

3. Williamson-Dickinson analysis

The model developed in Section 2 will be used to analyze the contribution to the rms error of the height field (or streamfield) when the model is updated with control data that differs in phase from the model predictions. The intention is to simulate real data insertion into a numerical prediction model, whose prediction capabilities are deficient because truncation is responsible for erroneous propagation of the allowable disturbance modes. The approach taken is similar to that used by Williamson and Dickinson (1972), hereafter referred to as W-D. The introduction of unbalanced initial data generates both gravity-inertia and quasigeostrophic wave modes, given by (24) and (26). In a numerical model, the gravity-inertia waves usually decrease rapidly in amplitude with time due to a removal mechanism characteristic of the particular model employed. W-D showed that the removal rate for the NCAR GCM is rapid during the first 6 h and less so thereafter. However, the wave energy in each of the six modes examined had been reduced by approximately 50% or more during the first 6 h and 35% or more during the first 4 h. Consequently, if updating is carried out, say, every 6 h, the ratio of gravity wave energy to quasi-geostrophic energy in mid-latitude flow should be relatively small. Yet there will be less error reduction from updating if gravity wave remnants have not been effectively eliminated before the next period of data assimilation. This type of error is considered to be small, particularly if the asymptotic error level, from updating, is reached in a relatively short time. In that case the accumulated error from gravity waves would remain relatively small. In the present model, as with that used by W-D, there is no gravity wave removal mechanism. These waves are simply removed from the data once the initial conditions are satisfied, i.e., they are not permitted to evolve. This approximation allows geostrophic adjustment to take place instantaneously, which is consistent with the fact that the initial conditions alone determine geostrophic and ageostrophic responses of the present model. It is not necessary to examine details of the adjustment process as long as it is essentially accomplished between updates.

The mathematical analysis is best illustrated by examining the case treated by W-D. Suppose the initial field is assumed to be geostrophically balanced, i.e.,

$$\mathbf{V}_i=\mathbf{k}\times\nabla\psi_i, \tag{34}$$

where **k** is a vertical unit vector; the assumed height field is represented by the geostrophic streamfunction

$$\psi_i = -Uy + \Psi_i e^{i(kx+ly)}, \tag{35}$$

and Ψ_i is a constant. Suppose the observed height field $\pi_i(x,y)$ is actually

$$\pi_i = -Uy + (1+\epsilon)\Psi_i e^{i(kx+ly)}, \tag{36}$$

where ϵ is an unspecified constant. It is desirable to use the information supplied by (36) to update the incorrect field. If ψ_i, given by (35), and π_i, given by (36), are substituted into (28), then

$$\frac{\lambda^2\hat{Z}}{\omega^2} = \epsilon\frac{\delta}{1+\delta}\Psi_i, \tag{37}$$

where $\delta=\lambda^2(k^2+l^2)$. Introduction of (36) and (37) into (33) yields the quasi-geostrophic height field after the first update:

$$\Pi^{(1)} = -Uy + \left[1+\epsilon\left(1-\frac{\delta}{1+\delta}\right)\right]\Psi_i e^{i(kx+\sigma\tau)+ily}. \tag{38}$$

Hereafter, it will be tacitly assumed that the ageostrophic field π is set equal to zero after each update has been performed. As noted by W-D, the corrected height differs from the true field by $\epsilon\Psi_i\delta/(1+\delta)$. At $\tau=\Delta\tau$, the predicted field is geostrophically balanced with $\psi_i=\Pi^{(1)}(x,y,\Delta\tau)$; the observed field has evolved so that

$$\pi_i = -Uy + (1+\epsilon)\Psi_i e^{i(kx+\sigma\Delta\tau)+ily}. \tag{39}$$

The predicted field is again updated with (39), leading to

$$\Pi^{(2)} = -Uy + \left[1+\epsilon\left(1-\left(\frac{\delta}{1+\delta}\right)^2\right)\right]\Psi_i e^{i(kx+\sigma\tau)+ily}. \tag{40}$$

If this process is repeated N times,

$$\Pi^{(N)} = -Uy + \left\{1+\epsilon\left[1-\left(\frac{\delta}{1+\delta}\right)^N\right]\right\} \times\Psi_i e^{i(kx+\sigma\tau)+ily}. \tag{41}$$

Eq. (41) shows that the model-predicted height approaches the observed height as the number of updates increases. If the true wind had been observed, then the geostrophic streamfunction $\Psi^{(N)}$ would be given by (41), with $\delta/(1+\delta)$ replaced by $1/(1+\delta)$. W-D assumed that the quasi-geostrophic mode was stationary but the present case, using a travelling wave, yields identical results.

The analysis just presented provides an *overly optimistic* view of the expected benefits from updating. First, the initial "shock" problem is avoided; second, a predictability error cannot arise because nonlinear interactions and dissipative processes are omitted and gravity waves are removed before the next update is accomplished; and finally, the case treated is equivalent to updating the model with data produced by the model itself—the problem of updating a numerical model with incompatible or observed data is not taken into consideration. This last problem will be analyzed in the following sections.

4. Phase error analysis

We assume that both the model and the atmosphere (subscript c) predict the evolution of Π by means of (8). However, the model and atmospheric dispersion relations differ:

$$\left.\begin{aligned}\sigma &= -\frac{k(U(k^2+l^2)-\beta)}{k^2+l^2+\lambda^{-2}}\\ \sigma_c &= -\frac{k(U(k^2+l^2)-\beta)}{k^2+l^2+\lambda_c^{-2}}\end{aligned}\right\}. \tag{42}$$

We may imagine that this difference, $\sigma\neq\sigma_c$, is brought about by truncation error or by means of an alteration of the true atmospheric structure by other model approximations. Consider, for example, that g may be replaced by effective gravity $g'=g\Delta\rho/\bar{\rho}$ within the framework of the present model, where $\bar{\rho}$ denotes the density of the bottom layer and $\Delta\rho>0$ is the density difference between the bottom layer and the inert top layer. In the "atmosphere"

$$(L\lambda_c)^2 = \frac{g_c' D_0}{f_0^2} = \frac{g\left(\frac{\Delta\rho}{\bar{\rho}}\right)_c D_0}{f_0^2} \sim \frac{g\left(\frac{\Delta T}{\bar{T}}\right)_c D_0}{f_0^2},$$

where density has been replaced by temperature T. In this case, model approximations that misrepresent the vertical structure of the atmosphere lead to phase propagation errors.

The analysis presented in Section 3 may be faithfully reproduced under the following conditions: The observed or control height field used for updating, satisfying (8), is given by

$$\Pi_c(x,y,\tau) = -Uy + (1+\epsilon)\Psi_i e^{i(kx+\sigma_c\tau)+ily}, \tag{43}$$

where σ_c is defined in (42). Updates, with (43), occur at times $\tau=n\Delta\tau$ ($n=1, 2, \ldots, N$), where $\Delta\tau=$constant.

The first update, at $\tau=T=0$, yields

$$\Pi^{(1)} = -Uy + \left[1+\epsilon\left(1-\frac{\delta}{1+\delta}\right)\right]\Psi_i e^{i(kx+\sigma\tau)+ily}, \tag{44}$$

which is identical with (38) because the phase difference is not apparent yet. At $\tau=\Delta\tau$, $\Pi_c(x,y,\Delta\tau)\neq\Pi^{(1)}(x,y,\Delta\tau)$. As a consequence, when Π_c is used to update at $\tau=\Delta\tau$

gravity waves are again generated at $T=0$. As before, these gravity waves are removed after the updating is accomplished. The second update yields

$$\Pi^{(2)}=-Uy+\left\{\frac{1+\epsilon}{1+\delta}e^{i\theta}+\frac{\delta}{1+\delta}\left[1+\epsilon\left(1-\frac{\delta}{1+\delta}\right)\right]\right\}\times\Psi_i e^{i(kx+\sigma\tau)+ily}, \quad (45)$$

where $\theta=(\sigma_c-\sigma)\Delta\tau$. For convenience, (45) may be expressed as

$$\Pi^{(2)}=-Uy+\left\{\frac{1+\epsilon}{1+\delta}\left[e^{i\theta}+\frac{\delta}{1+\delta}\right]+\left(\frac{\delta}{1+\delta}\right)^2\right\}\times\Psi_i e^{i(kx+\sigma\tau)+ily}. \quad (46)$$

The $\Pi^{(2)}$ field evolves according to (46) and, at $\tau=2\Delta\tau$, just prior to the next updates,

$$\Pi^{(2)}(2\Delta\tau)=-Uy+\left\{\frac{1+\epsilon}{1+\delta}e^{-i\theta}\left[1+\frac{\delta}{1+\delta}e^{-i\theta}\right]+\left(\frac{\delta}{1+\delta}\right)^2 e^{-2i\theta}\right\}\Psi_i e^{i(kx+\sigma_c 2\Delta\tau)+ily}. \quad (47)$$

This field (47) is now updated by $\Pi_c(2\Delta\tau)$, given by (43). A similar process may be repeated up to $\tau=N\Delta\tau$, at which time

$$\Pi^{(N)}(N\Delta\tau)=-Uy+\left\{\frac{1+\epsilon}{1+\delta}e^{-i\theta}\left[1+\frac{\delta}{1+\delta}e^{-i\theta}+\left(\frac{\delta}{1+\delta}\right)^2 e^{-2i\theta}+\cdots+\left(\frac{\delta}{1+\delta}\right)^{N-1}e^{-i(N-1)\theta}\right]+\left(\frac{\delta}{1+\delta}\right)^N e^{-iN\theta}\right\}\times\Psi_i e^{i(kx+\sigma_c N\Delta\tau)+ily}. \quad (48)$$

Since this form is applicable for wind updating as well as pressure updating, we define

$$a=\begin{cases}\dfrac{\delta}{1+\delta}: & \text{pressure updating}\\[2ex] \dfrac{1}{1+\delta}: & \text{wind updating}\end{cases} \quad (49)$$

where $\delta=\lambda^2(k^2+l^2)$ in each case. We now wish to determine the normalized amplitude error

$$r^{(N)}\equiv\left|\frac{(\Pi+Uy)-(\Pi_c+Uy)}{\Pi_c+Uy}\right|^{(N)}. \quad (50)$$

The expression $\Pi^{(N)}+Uy$, appearing in (50), is a complex series containing terms of the form $a^n\cos n\theta$ and $a^n\sin n\theta$. The sum is given by Jolly (1961, Series Nos. 454 and 455). The computation of $r^{(N)}$ is straightforward, but extensive, and the details are not presented. The final result is given by

$$r^{(N)}=\left\{r_M{}^2+2a^N(1-a)\left[\frac{\cos(N+1)\theta-\cos N\theta+0.5a^N(1-a)}{1-2a\cos\theta+a^2}\right]+\frac{2a^N}{1+\epsilon}\left[\frac{(1-a)[\cos(N-1)\theta-a\cos N\theta-a^N(\cos\theta-a)]}{1-2a\cos\theta+a^2}-\cos N\theta+0.5\frac{a^N}{1+\epsilon}\right]\right\}^{\frac{1}{2}}, \quad (51)$$

where r_M is the asymptotic error given by

$$r_M=\left(2\frac{1-\cos\theta}{1-2a\cos\theta+a^2}\right)^{\frac{1}{2}}, \quad (52)$$

and θ is defined in (45). This error r_M is only due to the difference in phase θ because the amplitude error ϵ disappears as $a^N\to 0$.

Consider first, properties of the asymptotic error r_M:

$$\left.\begin{array}{ll}
\text{(a)} & r_M\approx[2(1-\cos\theta)]^{\frac{1}{2}}\\
 & \quad=2\sin\theta/2, \quad a\ll 1\\
\text{(b)} & r_M\approx\dfrac{\theta}{1-a}, \quad \theta\ll 1, \quad a\neq 1\\
\text{(c)} & r_M\approx\theta, \quad a\ll 1, \quad \theta\ll 1\\
\text{(d)} & r_M=0, \quad \theta=2k\pi \quad (k=0,1,\ldots)\\
\text{(e)} & r_M\to 1 \text{ as } a\to 1, \quad \theta\neq 2k\pi\\
\text{(f)} & r_M|_{\max}=\left(\dfrac{2}{1+a}\right)^{\frac{1}{2}}
\end{array}\right\}. \quad (53)$$

when

$$a=\cos\theta, \quad 0<\theta\leqslant\pi/2 \ (\theta \text{ fixed})$$

These properties are illustrated in Figs. 3 and 4. A presentation of characteristic atmospheric parameter values will be deferred for the present. Next, $r^{(N)}$ is evaluated in order to determine the characteristic approach to the asymptotic state. Fig. 5 displays this information, for $a=0.5$ and indicated values of θ. This value of a, according to (37) and (49), corresponds to $\delta=\lambda^2(k^2+l^2)=1$. According to geostrophic adjustment theory, pressure updating should be more satisfactory than wind updating when $\kappa\lambda<1$, the reverse holding true when $\kappa\lambda>1$. In the former case, the wind field adapts to the pressure field; in the latter case, mass

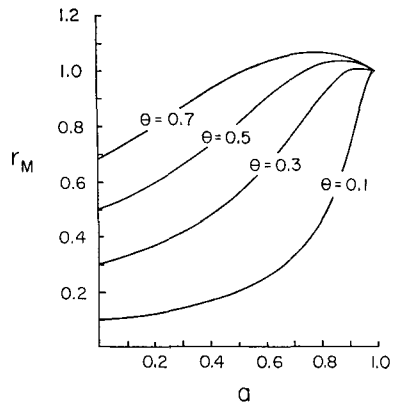

FIG. 3. Asymptotic error r_M as a function of a, defined by Eq. (49), for indicated phase errors θ.

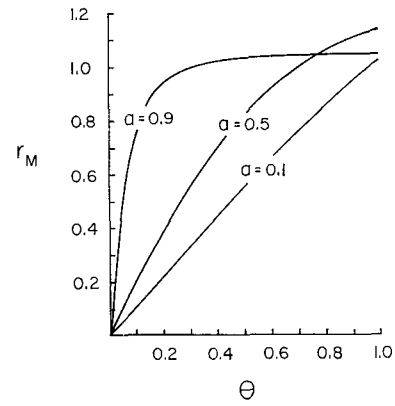

FIG. 4. Asymptotic error r_M as a function of phase error θ, for indicated values of a.

displacements bring the pressure field into adjustment with the wind field.

The initial error is determined by setting $N=0$ in (51) to obtain $r^{(0)}=\epsilon/(1+\epsilon)$. The values $\epsilon=0$, 1, used in Fig. 5, could be expected to be approximate lower and upper limits of observational errors. The response, illustrated in Fig. 5, is typical of the time-dependent approach to the asymptotic error r_M exhibited by other values of a. The asymptotic error is independent of the initial error, in agreement with Williamson's (1973) numerical experiments shown in Figs. 1 and 2. One-to-one correspondence between the present results and Williamson's computations cannot be made because his rms error has not been normalized, and the numerical model admits a broad spectrum of waves. Nevertheless, the principal features that characterize the effect of truncation error in the numerical model seem to be well reproduced by the present analysis. The agreement appears to be best in the range $0.1\lesssim\theta\lesssim0.2$. Suppose we assume that $\Delta\tau=12$ h and $\lambda=[(g\Delta\rho/\tilde{\rho})D_0]^{\frac{1}{2}}/f_0\approx10^3$ km for $D_0\approx8$ km and $f_0\approx10^{-4}$ sec^{-1}. Then $[(\sigma_c-\sigma)/k]k\approx[(\sigma_c-\sigma)/k]\lambda^{-1}\approx2\theta$ (day)$^{-1}$. The difference in phase

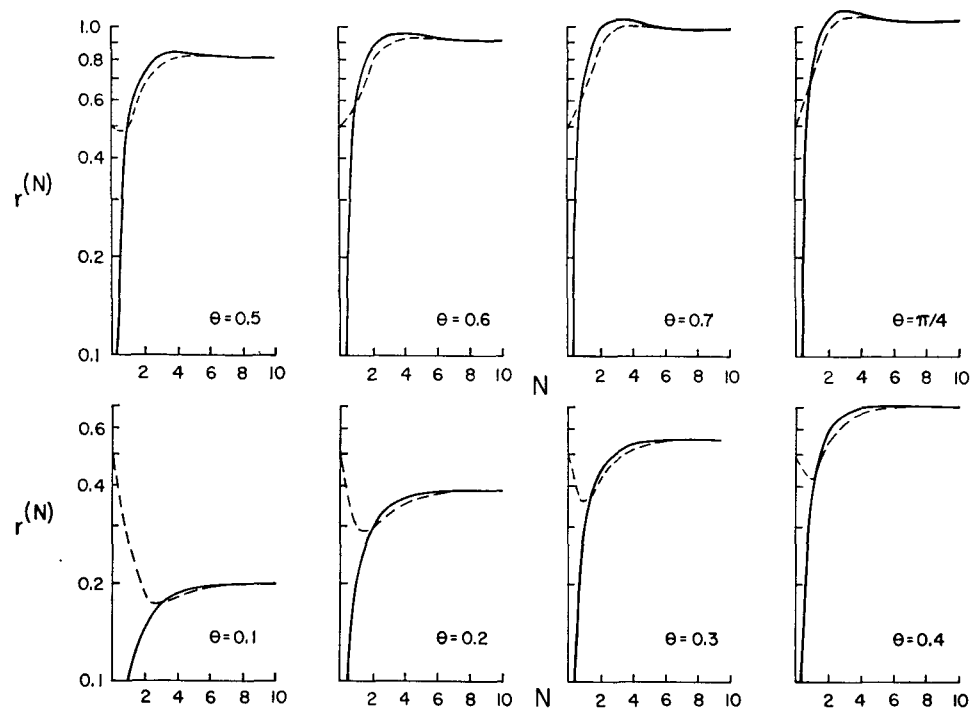

FIG. 5. Normalized error $r^{(N)}$, given by Eq. (51), as a function of updates performed N. In all cases displayed, $a=0.5$. The initial amplitude errors are $\epsilon=0$ (solid) and $\epsilon=1.0$ (dashed).

TABLE 1. Average number of updates N^* needed to attain $|1-r^{(N)}/r_M| \leq 0.05$, where $r^{(N)}$ and r_M are defined by (51) and (52). Eight values ($0.1 \leq \theta \leq \pi/4$) were used to determine N^* and the maximum deviation from this average value, $\Delta = N - N^*$.

a	0.1	0.2	0.3	0.4	0.5	0.6	0.7	0.8	0.9
N^*	2	2	3	3	4	5	7	12	27
Δ	0	0	−1	−1	±1	±1	±1	±1	+2

propagation speed is

$$\frac{\sigma_c - \sigma}{k} \approx 2\theta \times 10^3 \text{ km day}^{-1},$$

which corresponds to about 200 and 400 km day^{-1} when $\theta = 0.1$ and 0.2. Although Williamson has not indicated the magnitude of the propagation errors, due to truncation in his experiment, the values given above fall in the range determined by Miyakoda *et al.* (1972) using the GFDL GCM. It would be expected that the NCAR GCM would yield errors of a similar magnitude.

The results presented in Fig. 5 reveal two interesting characteristics. In the range $0.1 \lesssim \theta \lesssim 0.5$, there is an initial error reduction. This initial tendency reflects the ability of the model to recover the correct field, as shown by (41), when $\theta \equiv 0$. However, the phase error ultimately overwhelms this initial tendency, causing a dip in the error curve, and the asymptotic error level is rapidly attained. When $\theta > 0.5$, the relatively large phase error dominates the evolution of the error. It is also noted that the length of time necessary to attain the asymptotic error level depends only on the number of updates and is independent of $\Delta\tau$. (It has been assumed that $\Delta\tau \gtrsim 6$ h.) When $a < 0.5$ the error curves are very similar to those in Fig. 5, but the slight overshoot of the asymptotic error, shown for $\theta \gtrsim 0.4$, is less pronounced; when $a > 0.5$, the overshoot is more pronounced and two or three damped oscillations occur.

Table 1 shows the average number of updates N^*, required to reach to within $\pm 5\%$ of the asymptotic error r_M, as a function of a. For practical purposes N^* is independent of θ. This feature is indicated by the relatively small amount of scatter, for different values of θ, indicated by $\Delta = N - N^*$. Characteristic scales of the geostrophic modes are shown in Table 2. We note that for almost all scales, characteristic of mid-latitude flow, the asymptotic error level may be reached within about 3–4 days even with data assimilation every 12 h. However, Fig. 3 and 4, or (52), show that r_M is relatively small only if a and θ are both small. Consequently, error reduction can only be accomplished, for a given a, by reducing the magnitude of θ. In this regard, it is necessary to update as frequently as possible, and, equally important, to reduce the effect of truncation on the principal energy containing modes.

TABLE 2. Characteristic scales of the geostrophic modes (km), at latitudes 30°, 45° and 60°. The left-hand column corresponds to pressure updating and the right-hand column to wind updating, as indicated in Eq. (49). $\lambda(30) = 1400$ km, $\lambda(45) = 1000$ km, $\lambda(60) = 816$ km, and $\delta = \lambda^2(k^2+l^2) = (2\pi\lambda/L)^2$.

Pressure		Latitude			Wind	
a	δ	30°	45°	60°	δ	a
0.1	0.111	26,390	18,850	15,380	0.111	0.9
0.5	1.000	8,800	6,280	5,130	1.000	0.5
0.9	9.000	2,930	2,090	1,710	9.000	0.1

5. Static initialization

The simple replacement of the geostrophic forecast value Π by the geostrophic control value Π_c is referred to as "static initialization." If at time $\tau = 0$, (26) is replaced by (43), then Π evolves according to

$$\Pi^{(1)} = -Uy + (1+\epsilon)\Psi_i e^{i(kx+\sigma\tau)+ily}. \tag{54}$$

At time $\Delta\tau$, $\Pi^{(1)}$ is replaced again by (43) and we obtain

$$\Pi^{(2)} = -Uy + (1+\epsilon)\Psi_i e^{i\theta} e^{i(kx+\sigma\tau)+ily}. \tag{55}$$

Repeated updating with (43) yields

$$\Pi^{(N)}(N\Delta\tau) = -Uy + (1+\epsilon)\Psi_i e^{(N-1)i\theta} e^{i(kx+\sigma N\Delta\tau)+ily}. \tag{56}$$

The error, prior to any update, is given by

$$r = \left| \frac{(\Pi + Uy) - (\Pi_c + Uy)}{\Pi_c + Uy} \right|^{(N)} = [2(1-\cos\theta)]^{\frac{1}{2}} = 2\sin\theta/2. \tag{57}$$

We now consider the ratio

$$\frac{r}{r_M} = (1 - 2a\cos\theta + a^2)^{\frac{1}{2}}, \tag{58}$$

where r_M is given by (52). As a result, static initialization leads to a smaller error if $\cos\theta > a/2$, which is always satisfied if $0 \leq \theta < \pi/3$. We are led to the conclusion that static initialization of a quasi-geostrophic model, without allowing an adjustment process to occur, is a better updating procedure than the procedure adopted in Section 4. The two procedures are essentially equivalent when $a \ll 1$. In practice, however, quasi-geostrophic models have generally been replaced by primitive equation prediction models because the former are generally limited, compared to the latter, in predictive capabilities. Consequently, only the method of Section 4 will be used hereafter.

6. Random phase errors

Phase differences between the model and atmospheric disturbance modes would not be expected to remain constant during the total period of data assimila-

tion. Moreover, the propagation error for each allowable mode depends on wavenumber and space increment used in the finite-difference calculation. The previous analysis, in Section 4, can be adapted to include some of these effects in a relatively simple manner. The inconstancy of the phase error may be modelled by specifying the phase variable, $\theta=(\sigma_c-\sigma)\Delta\tau$, as a random variable. This approach could, in a crude sense, be interpreted as a simulation of a model disturbance whose propagation speed is not constant relative to the control or atmospheric disturbance due to nonlinearities, inhomogeneous boundary conditions or thermal forcing, etc. We may also interpret this approach as a model of *asynoptic* data assimilation, if we view $\Delta\tau$ as a random variable while holding $\sigma_c-\sigma$ constant.

The approach taken here is based on an analysis by MacFarlane (1949), who computed the energy spectrum of an almost periodic succession of pulses in which the irregularity occurs in a random way. Application to automatic control and signal processing systems was intended. However, the approach is quite general and Blumen (1965) used a similar analysis to model mountain lee-wave drag produced by irregularly spaced orography.

To begin, we define

$$\theta_n=n\langle\theta\rangle+\theta_n', \tag{59}$$

where n indicates any updating time $\tau=n\Delta\tau$, $\langle\theta\rangle$ is a constant, and θ' is a random phase error; θ_n may be inserted into (48) in place of $n\theta$ and the steps leading to $r^{(N)}$, as expressed by (50), carried out. Next we determine the probability average

$$\langle(r^2)^{(N)}\rangle=\int_{\theta_n|\min}^{\theta_n|\max}(r^2)^{(N)}p(\theta_n)d\theta_n, \tag{60}$$

where $p(\theta_n)$ is the probability density function of the random variable θ_n and the integration is carried out between the minimum and maximum values of θ_n. The above integration is carried out under the assumption that statistical independence exists between the deviations from the mean phase error $\langle\theta\rangle$. This assumption implies that, for every integer n and m,

$$\left\langle\sum_{n=0}^{N-1}\sum_{m=0}^{M-1}\{\langle f(\theta_n)\rangle+[f(\theta_n)-\langle f(\theta_n)\rangle]\}\times\{\langle f(\theta_m)\rangle+[f(\theta_m)-\langle f(\theta_m)\rangle]\}\right\rangle$$
$$=\langle[\sum_{n=0}^{N-1}\langle f(\theta_n)\rangle]^2\rangle+\langle\sum_{n=0}^{N-1}[f(\theta_n)-\langle f(\theta_n)\rangle]^2\rangle, \tag{61}$$

where $f(\theta_n)$ is any function of θ_n. It is further assumed that all deviations from $\langle\theta\rangle$ are equally probable between the limits $\pm\alpha$. This distribution may be expressed as

$$\left.\begin{aligned}p(\theta_n)&=\frac{1}{2\alpha}, \quad |\theta_n|\leqslant\alpha\\ p(\theta_n)&=0, \quad |\theta_n|>\alpha\end{aligned}\right\}. \tag{62}$$

The essential integrations have been presented by Blumen (1965). The expected value of the asymptotic error is given by

$$E(r_M)=(\lim_{N\to\infty}\langle(r^2)^N\rangle)^{\frac{1}{2}}$$
$$=\left\{\left(1+\frac{1-a}{1+a}\right)\left[1-\left(\frac{\sin\alpha}{\alpha}\right)^2\right]+r_M^2\left(\frac{\sin\alpha}{\alpha}\right)^2\right\}^{\frac{1}{2}}, \tag{63}$$

where a is given by (49) and α by (62). Note that r_M [(52)] is recovered when $\alpha=0$. The maximum deviation $|\alpha|$ would not exceed $\langle\theta\rangle/2$ if $\Delta\tau$ is treated as the random variable. If $\langle\theta\rangle=1$, a relatively large phase error, then $|\alpha|\leqslant 0.5$. In this case, the first two terms of the series

$$\frac{\sin\alpha}{\alpha}=1-\frac{\alpha^2}{3!}+\cdots$$

yield a sufficiently accurate representation. $E(r_M)$ may now be expressed as

$$E(r_M)\approx r_M\left[1+\frac{2}{(1+a)r_M^2}\frac{\alpha^2}{3}\right]^{\frac{1}{2}}. \tag{64}$$

Consider $\langle\theta\rangle\lesssim 0.2$, corresponding to a maximum propagation error of order 400 km day^{-1} in mid-latitudes, if $\Delta\tau=12$ h. Then, from (53b),

$$r_M\approx\frac{\langle\theta\rangle}{1-a}, \quad a<1. \tag{65}$$

Consequently, if we assume that $\alpha=\langle\theta\rangle/2$, then (64) reduces to

$$E(r_M)\approx\frac{\langle\theta\rangle}{1-a}\left[1+\frac{1}{12}\frac{(1-a)^2}{1+a}\right]. \tag{66}$$

We may conclude that in the range of phase differences that generally occur between short-term numerical predictions and the observed state, random variations in phase will add an additional random "noise" error of order 8% or less.

If we consider that the randomness introduced in (59) is inherent in $\Delta\tau$ rather than in $\sigma_c-\sigma$, then (66) shows that *asynoptic data assimilation on a purely random basis increases the asymptotic error level.*

7. Amplitude variation

An analysis may be carried out when the observed or control field is represented by

$$\Pi_c=-Uy+(1+\epsilon)\Psi_i$$
$$\times[e^{i(k_1x+\sigma_1\tau)+il_1y}+e^{i(k_2x+\sigma_2\tau)+il_2y}], \tag{67}$$

where $k_1^2+l_1^2=k_2^2+l_2^2$, and

$$\left.\begin{aligned}\sigma_1&=-k_1\frac{[U(k_1^2+l_1^2)-\beta]}{k_1^2+l_1^2+\lambda_c^{-2}}\\ \sigma_2&=-k_2\frac{[U(k_2^2+l_2^2)-\beta]}{k_2^2+l_2^2+\lambda_c^{-2}}\end{aligned}\right\}. \tag{68}$$

It may be verified that (67) and (68) satisfy (8) because the nonlinear terms sum to zero. It is assumed that $\sigma_1\neq\sigma_2(k_1\neq k_2,\ l_1\neq l_2)$ but, according to (68), the phase speed of each wave is the same. Then Π_c may be written as

$$\begin{aligned}\Pi_c=&-Uy+2(1+\epsilon)\Psi_i\\ &\times\cos\tfrac{1}{2}[(k_1-k_2)x+(l_1-l_2)y+(\sigma_1-\sigma_2)\tau]\\ &\times\exp\left\{\frac{i}{2}[(k_1+k_2)x+(\sigma_1+\sigma_2)\tau]+\frac{i}{2}(l_1+l_2)y\right\}.\end{aligned} \tag{69}$$

In the form (69), it is apparent that Π_c may be represented in terms of a wave of approximately the same wavelength and frequency as in (43), if $k_1\sim k_2$, $l_1\sim l_2$, but with a *spatially varying amplitude.* The wave system, (67) or (69), translates without change of shape at a constant rate $c=(\sigma_1-\sigma_2)/(k_1-k_2)=(\sigma_1+\sigma_2)/(k_1+k_2)$.

The model field evolves according to

$$\begin{aligned}\Pi=&-Uy+2\Psi_i\\ &\times\cos\tfrac{1}{2}[(k_1-k_2)x+(l_1-l_2)y+(\sigma_1'-\sigma_2')\tau]\\ &\times\exp\left\{\frac{i}{2}[(k_1+k_2)x+(\sigma_1'+\sigma_2')\tau]+\frac{i}{2}(l_1+l_2)y\right\},\end{aligned} \tag{70}$$

where σ_1' and σ_2' are given by (68) with λ^2 replacing λ_c^2. As before, a phase error exists between the control state and the model predictions. In the present case, however, a phase error exists between each wave.

The analysis proceeds as in Section 4. Since $k_1^2+l_1^2=k_2^2+l_2^2$, $\delta_1=\delta_2=\delta$, where δ is defined in (49). This circumstance means that $\Pi^{(N)}(N\Delta\tau)$ may be written as in (48):

$$\begin{aligned}\Pi^{(N)}(N\Delta\tau)=&-Uy+\left\{\frac{1+\epsilon}{1+\delta}e^{-i\theta_1}\right.\\ &\times\left[1+\frac{\delta}{1+\delta}e^{-i\theta_1}+\cdots+\left(\frac{\delta}{1+\delta}\right)^{-N1}e^{-i(N-1)\theta_1}\right]\\ &\left.+\left(\frac{\delta}{1+\delta}\right)^{N}e^{-iN\theta_1}\right\}\Psi_i e^{i(k_1x+\sigma_1\tau)+il_1y}\\ &+\left\{\frac{1+\epsilon}{1+\delta}e^{-i\theta_2}\left[1+\frac{\delta}{1+\delta}e^{-i\theta_2}\right.\right.\\ &\left.\left.+\cdots+\left(\frac{\delta}{1+\delta}\right)^{N-1}e^{-i(N-1)\theta_2}\right]+\left(\frac{\delta}{1+\delta}\right)^{N}e^{-iN\theta_2}\right\}\\ &\times\Psi_i e^{i(k_2x+\sigma_2\tau)+il_2y},\end{aligned} \tag{71}$$

where σ_1 and σ_2 are given by (68) and

$$\left.\begin{aligned}\theta_1&=\sigma_1-\sigma_1'\\ \theta_2&=\sigma_2-\sigma_2'\end{aligned}\right\}. \tag{72}$$

Again, the computation of $r^{(N)}$ is a straightforward and extensive procedure. However, since two waves are present, the mean error is defined as

$$(\overline{[r^2]^{(N)}})^{\frac{1}{2}}=\left(\frac{1}{L_xL_y}\int_0^{L_y}\int_0^{L_x}[r^2]^{(N)}dxdy\right)^{\frac{1}{2}}, \tag{73}$$

where $L_x=2\pi/(k_1-k_2)$ and $L_y=2\pi/(l_1-l_2)$. The limiting value is

$$\begin{aligned}&\lim_{N\to\infty}(\overline{[r^2]^{(N)}})^{\frac{1}{2}}\\ &=\overline{r_M}=\left(\frac{1-\cos\theta_1}{1-2a\cos\theta_1+a^2}+\frac{1-\cos\theta_2}{1-2a\cos\theta_2+a^2}\right)^{\frac{1}{2}},\end{aligned} \tag{74}$$

which reduces to (52) when $\theta_1=\theta_2=\theta$. (The cross-product terms vanish by virtue of the averaging process.)

An average error, due to the presence of two waves, may be defined as

$$(r_M)_{\text{ave}}\equiv\tfrac{1}{2}(r_1+r_2), \tag{75}$$

where

$$\left.\begin{aligned}r_1&=\left(2\frac{1-\cos\theta_1}{1-2a\cos\theta_1+a^2}\right)^{\frac{1}{2}}\\ r_2&=\left(2\frac{1-\cos\theta_2}{1-2a\cos\theta_2+a^2}\right)^{\frac{1}{2}}\end{aligned}\right\}. \tag{76}$$

If (74) and (75) are both squared and compared, it is clear that

$$\overline{r_M}\geqslant(r_M)_{\text{ave}}, \tag{77}$$

where equality implies $\theta_1=\theta_2$. It may be concluded, from (77), that an additional loss of information occurs. In essence, the out-of-phase error between the control and model states is enhanced as a result of the spatial variation of the amplitudes of each wave field.

If we consider $\theta_1=0.1$, $\theta_2=0.2$ and $a=0.5$ as typical values, then $r_1=0.198$ and $r_2=0.384$. As a consequence, we obtain $\bar{r}_M=0.306$ and $(r_M)_{\text{ave}}=0.291$. In this case, the error increases by 5.1%. The importance of this type of error in data assimilation will again depend on how faithfully the principal energy bearing modes, described by the model, represent the true atmospheric state.

8. Summary and remarks

The present simple model appears to explain significant features of forecast error that arise due to

truncation and, perhaps, also due to incorrect parameterization of physical process. The latter conjecture bears further investigation along the lines initiated by Williamson and Kasahara (1971). The sole source of error in the present analysis is assumed to be associated with phase differences between the modes of the numerical model and the observed atmospheric state. The existence of such phase differences has been well-established by theoretical analysis and by numerical experimentation. Within the context of the present analysis, the forecast error will be further enhanced if the phase error varies with time, in a more or less random manner, or if the amplitude of the wave system has a spatial variation. A corollary is that asynoptic data assimilation carried out on a random basis could increase the asymptotic error level by addition of a random noise error to the mean error level.

A significant reduction in the rms forecast error should be attainable by a reduction in the phase error. The difference in propagation speeds between the model and the atmospheric state must be reduced or the increments $\Delta\tau$ between updates must be reduced, or both. There is a lower limit to $\Delta\tau$, however, below which error reduction may not be realized because gravity waves have not been sufficiently reduced in amplitude. The practical limit appears to be $\Delta\tau\sim 6$ h. Moreover, a significant reduction in phase speed differences, associated with truncation, may be difficult to achieve. Experiments with increased resolution, higher-order differencing and with spectral representations indicate that improved forecast accuracy is possible, yet no ideal grid system exists for global or hemispheric forecasts (Döös, 1970).

Although the present model results are directed to mid-latitude features, it appears that data assimilation in tropical latitudes will yield limited, if any, success. In view of the broader spectral energy distribution in the tropical atmosphere, Holton (1969) has suggested that the full primitive equations be used and, moreover, that fine vertical resolution be employed to insure that vertically propagating modes are well represented. On this basis, it would appear that truncation error will be a more serious problem in models of the tropical circulation, since forecast accuracy will be very sensitive to the vertical as well as the horizontal resolution. Due to the quasi-geotrophic character of the flow, forecast errors are perhaps less sensitive to the vertical resolution in mid-latitude models.

Nonetheless, the vertical structure should be an important consideration in updating mid-latitude meteorological fields. Phase errors may be examined by using a vertically stratified fluid model. If the approach of Section 4 is followed, the time evolution of the quasi-geostrophic flow is determined by specifying ψ_i, π_i and T_i at the initial time. An error analysis may be carried out when either one or two of these variables are specified initially and at each update period. In this regard, the dependence between the forecast error and the number of levels, as well as their position in space, over which data are assimilated may also be considered.

The present approach may also be readily adapted to examine other problems in data assimilation. For example, predictability error growth may be studied by using a truncated series of eigenfunctions, describing some basic features of the synoptic-scale motion, in order to solve (8). This latter method of solution, used by Lorenz (1960), is relatively uncomplicated at the first update period. However, nonlinear interactions broaden the spectrum of motions after each update. Although numerical computations will undoubtedly be required to complete the solution, this approach is less cumbersome than an extended integration of a fully nonlinear model.

In conclusion, it is suggested that relatively simple analytical and numerical modelling studies be undertaken to help establish priorities for numerical experimentation with more complex models, and to help make the interpretation of the results more accessible.

Acknowledgments. Interpretation of the NCAR GCM numerical experiments was aided by discussions with David L. Williamson, who also supplied Figs. 1 and 2 in the text. I am also grateful to Akira Kasahara for reading the manuscript and providing helpful criticism. This investigation was supported by the Atmospheric Science Section of the National Science Foundation, under Grant GA-31868.

APPENDIX

Derivation of the Energy Equation

Eq. (21) may be established directly from the energy equation for the shallow water equations:

$$\frac{\partial}{\partial t}\int\int_{S_*}\frac{1}{2}\left\{\left(1+\frac{h_*}{D_0}\right)(u_*^2+v_*^2)+g\frac{h_*^2}{D_0}\right\}dx_*dy_*=0, \quad \text{(A1)}$$

where the variables are defined in (2). Nondimensionalization and introduction of (4) produces

$$\left(\frac{\partial}{\partial T}+\mathrm{Ro}\frac{\partial}{\partial \tau}\right)\int\int_S \tfrac{1}{2}[(1+\lambda^{-2}\,\mathrm{Ro}\pi)\times(u^2+v^2)+\lambda^{-2}\pi^2]dxdy=0, \quad \text{(A2)}$$

where Ro and λ are defined by (1) and (3). A power series expansion in Ro yields, to zero- and first-order,

$$\frac{\partial}{\partial T}\frac{1}{2}\int\int_S (u_0^2+v_0^2+\lambda^{-2}\pi_0^2)dxdy=0, \quad \text{(A3)}$$

$$\frac{\partial}{\partial T}\int\int_S\left[\lambda^{-2}\frac{\pi_0}{2}(u_0^2+v_0^2)+u_0u_1+v_0v_1+\lambda^{-2}\pi_0\pi_1\right]dxdy$$
$$+\frac{\partial}{\partial\tau}\frac{1}{2}\int\int_S(u_0^2+v_0^2+\lambda^{-2}\pi_0^2)dxdy=0. \quad \text{(A4)}$$

As noted in (20), an integral of (A3) is

$$\mathcal{E}(\tau)=\frac{1}{2}\int\int_S(U^2+V^2+\lambda^{-2}\Pi^2$$
$$+u^2+v^2+\lambda^{-2}\pi^2)dxdy. \quad \text{(A5)}$$

As a consequence, $\partial\mathcal{E}/\partial\tau$ in (A4) must be set equal to zero in order to avoid unbounded growth in T. This last step establishes (21).

REFERENCES

Blumen, W., 1965: A random model of momentum flux by mountain waves. *Geofys. Publ.*, **26**, 33 pp.

——, 1972: Geostrophic adjustment. *Rev. Geophys. Space Phys.*, **10**, 485–528.

Cole, J. D., 1968: *Perturbation Methods in Applied Mathematics.* Blaisdell, 260 pp.

Craig, R. A., 1945: A solution of the nonlinear vorticity equation for atmospheric motion. *J. Meteor.*, **2**, 175–178.

Döös, B. R., 1970: Numerical experimentation related to GARP. GARP Publ. Ser. No. 6, WMO-ICSU-Joint Organizing Committee, 68 pp.

Hayden, C. M., 1973: Experiments in the four-dimensional assimilation of Nimbus 4 SIRS data. *J. Appl. Meteor.*, **12**, 425–436.

Holton, J. R., 1969: A note on scale analysis of tropical motions. *J. Atmos. Sci.*, **26**, 770–771.

Jastrow, R., and M. Halem, 1973: Simulation studies and the design of the first GARP global experiment. *Bull. Amer. Meteor. Soc.*, **54**, 13–21.

Jolly, L. B. W., 1961: *Summation of Series.* Dover, 251 pp.

Kasahara, A., 1972: Simulation experiments for meteorological observering systems for GARP. *Bull. Amer. Meteor. Soc.*, **53**, 252–264.

Kurihara, Y., 1965: On the use of implicit and iterative methods for the time integration of the wave equation. *Mon. Wea. Rev.*, **93**, 33–46.

Lorenz, E. N., 1960: Maximum simplification of the dynamic equations. *Tellus*, **12**, 243–254.

MacFarlane, G. G., 1949: On the energy spectrum of an almost periodic succession of pulses. *Proc. IRE*, **37**, 1139–1143.

Miyakoda, K., R. F. Strickler, C. J. Nappo, P. L. Baker and G. D. Hembree, 1971: The effect of horizontal grid resolution in an atmospheric circulation model. *J. Atmos. Sci.*, **28**, 481–499.

——, G. D. Hembree, R. F. Strickler and I. Shulman, 1972: Cumulative results of extended forecast experiments. 1. Model performance for winter cases. *Mon. Wea. Rev.*, **100**, 836–855.

Neamtan, S. M., 1946: The motion of harmonic waves in the atmosphere. *J. Meteor.*, **3**, 53–56.

Williamson, D. L., 1973: The effect of forecast error accumulation on four-dimensional data assimilation. *J. Atmos. Sci.*, **30**, 537–543.

——, and R. E. Dickinson, 1972: Periodic updating of meteorological variables. *J. Atmos. Sci.*, **29**, 190–193.

——, and A. Kasahara, 1971: Adaptation of meteorological variables forced by updating. *J. Atmos. Sci.*, **28**, 1313–1324.